Technical Report

TR-11-09

Effect of loading rate on creep of phosphorous doped copper

Henrik C.M. Andersson-Östling, Rolf Sandström
Swerea KIMAB

December 2011

Svensk Kärnbränslehantering AB
Swedish Nuclear Fuel
and Waste Management Co

Box 250, SE-101 24 Stockholm
Phone +46 8 459 84 00

ISSN 1404-0344
SKB TR-11-09

Effect of loading rate on creep of phosphorous doped copper

Henrik C.M. Andersson-Östling, Rolf Sandström
Swerea KIMAB

December 2011

Abstract

Creep testing of copper intended for nuclear waste disposal has been performed on continuous creep tests machines at a temperature of 75°C. The loading time has been varied from 1 hour to 6 months. The rupture strain including both loading and creep strains does not differ from traditional dead weight lever creep test rigs. The loading strain increases with increasing loading time, at the expense of the creep strain.

The time dependence of the creep strain has been modelled taking athermal plastic deformation and creep into account. During loading the contribution to the strain from the athermal plastic deformation dominates until the stress is close to the constant load level. When the constant load has been reached there is no more athermal strain and all of the strain comes from creep.

Contents

1 Background

Spent nuclear fuel from the Swedish nuclear power plants is planned to be encapsulated in canisters and placed in a repository 500 m down in stable bedrock. Details of the repository are given in [1] and only a brief summary is given below. The canisters consist of an inner load bearing cast iron structure with square holes for the spent fuel elements and an outer copper shell. A steel lid is mounted after the fuel is emplaced in the canister. A copper lid is placed on top of the tube and closed by friction stir welding. Due to geometrical constraints it is not possible to have a press fit between the iron and the copper, but instead a gap of 3 mm is left between the two. Initially the canister will have a temperature of max 100°C. The temperature will be gradually reduced over many centuries eventually reaching room temperature. Over a long period of time (but generally shorter than for the cooling) the bentonite clay surrounding the canisters will become saturated with groundwater, and the hydrostatic pressure will increase. Due to this pressure the gap between the cast iron and the copper will close, since the copper will deform by creep. Much research effort has been spent on the creep properties of the copper intended for the canisters. The results have shown [2] that the creep ductility is large enough to cope with the projected deformations established by simulations of the process [3].

The testing supporting this research has all been performed using standard creep testing methods. This includes an application of the load as fast as possible without loading shock (it takes about 3 minutes), as the relevant standard states [4]. Traditional creep test rigs also have a maximum travel of some 5 mm before the load arm has to be reset. During the reset the load is temporarily lifted from the specimen and then reapplied. This reapplication appears on the creep results as a new primary creep stage, affecting the overall result of the creep test.

In the repository the creep load will be applied slowly over a very long period as mentioned above without unloading at any stage. It is therefore vital that the creep testing emulates these conditions as closely as possible. The work presented here is aimed at studying the creep response of oxygen free, phosphorous doped copper (Cu-OFP) under continuous, unbroken long term application of the creep load.

2 Experimental

The experiments in this work have been performed on newly developed creep tests rigs without the traditional loading arm, Figure 2-1 and Figure 2-2. The loading arm has been replaced by a step motor actuating on the specimen through a gearbox and an angled gear. In the load line a load cell is incorporated and the step motor is controlled by feedback from the load cell. An in-house developed computer programme controls the test and allows for application of the load in a preset time. For calibration purposes the load cell is coupled to a calibration load cell before testing to ensure correct load. In the present work, the load is applied linearly with time, and the longest application tested is 6 months. The load during the creep phase of the test is controlled to within 1 N. The furnace is of the hot air type and the temperature during the test is controlled to within ± 1°C.

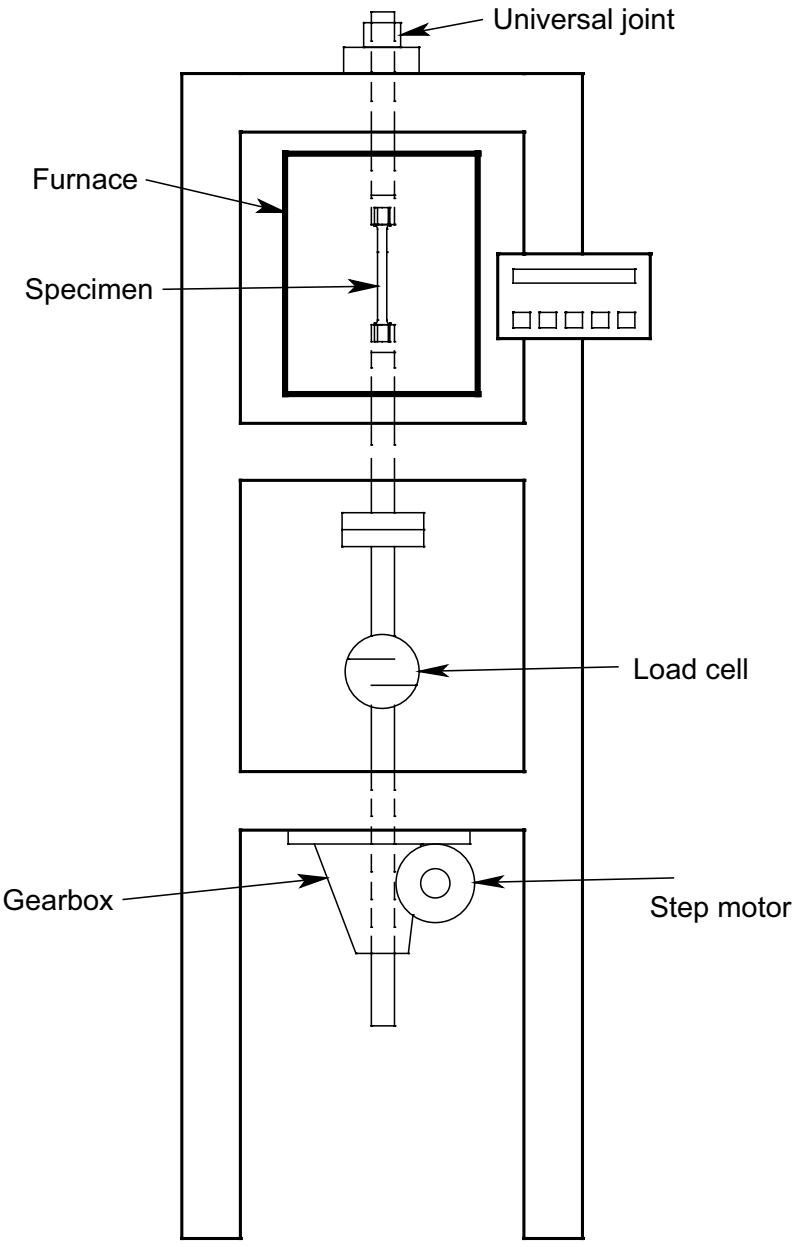

Figure 2-1. *Schematic drawing of the load controlled creep test rig.*

Figure 2-2. *Image of the completed test rigs in the laboratory.*

Since the strain of the specimen cannot be measured by extensometers attached to the specimen itself, the solution used was to measure strain outside the furnace. An extensometer was affixed to the load rod below the load cell and the strain measured to within 100 nm. Since the strain measured here includes strains in the load rods and the test rig itself, a phenomenon called the compliance of the test rig has to be compensated for. Before testing commenced a dummy steel specimen that does not deform was mounted in place of the copper specimen. The load was then applied to the test rig and the resulting strain was logged for each load increment. A compensating mathematical expression was obtained and this was then applied to the real tests yielding the correct strain on the specimen.

Standard creep test specimens with a gauge length of 50 mm and a diameter of 5 mm were used, Figure 2-3. These were taken from a forged copper lid delivered to Swerea KIMAB for this purpose with the SKB identity L21/TX104. The chemical analysis is given in Table 2-1 and Table 2-2. After machining the specimens were subjected to an annealing step to remove all cold work that could have been introduced inadvertently during the previous step. The anneal was for 5 minutes at 600°C followed by water quenching. Previous experience has shown this treatment to completely remove cold work without introducing any grain growth [5]. In addition to the annealed specimens three unannealed specimens were tested for comparison.

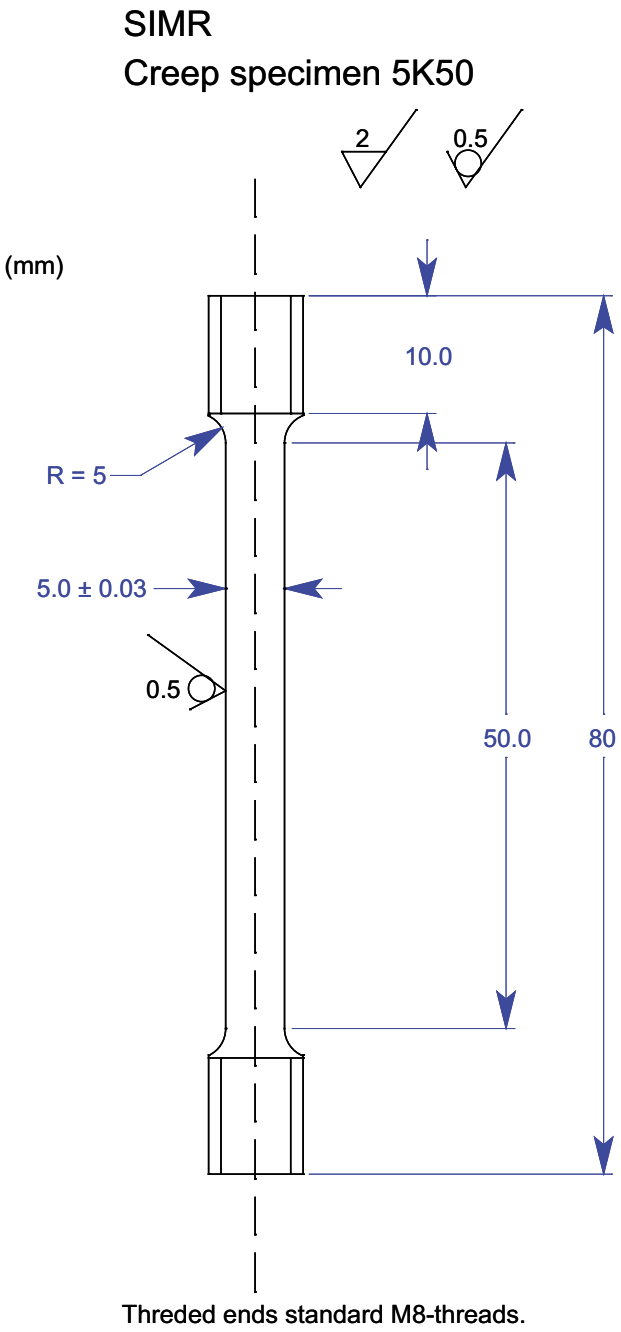

Figure 2-3. *The creep test specimen used.*

Table 2-1. Chemical analysis for the lid L21/TX104 (ppm).

Cast	Pb	Bi	As	Sb	Sn	Zn	Mn	Cr	Co	Cd	Fe	Ni	Ag	Se	Te	S
L760	<1	<1	<1	1	<0.5	<1	<0.5	<1	<1	<1	2	2	13	<1	<1	5

Table 2-2. Chemical analysis and properties for the lid L21/TX104.

Cast	Electrical conductivity [m/Ω mm^2]	P [ppm]	O_2 [ppm]	Density [g/cm^3]
L760	56.1–56.7	45–60	1–2	8.91–8.92

3 Results

The results from the testing and the test matrix are given in Table 3-1 and in graphical form in Figure 3-1 and Figure 3-2. In the latter image the total time including loading time is given. For comparison the results from similar material using traditional creep testing is included in the graphs. The traditional tests were performed using a loading time of about 2 minutes and also included several resets when the specimen was temporarily unloaded. The slow loading tests were performed with 1 hour as the fastest loading time, i.e. approximately 2 orders of magnitude faster than in the traditional tests. It should be noted that the previous testing was performed using 10 mm specimens as opposed to 5 mm in the present investigation, and the specimens were not annealed.

A total of 14 specimens were tested at 75°C and most were allowed to rupture. One specimen experienced an overload during the creep stage and has been removed. After initial tests at 180, 175 and 170 MPa, the standard stress was selected as 165 MPa. Several loading times were used at this stress from 1 hour as the shortest one up to 6 months. The Norton exponent given by the power law, Equation 3-1, is difficult to evaluate from the tests due to the small range in applied stress but was found to be 114 for the annealed tests, well into the power law break-down area.

$$\dot{\varepsilon} = A\sigma^n \tag{3-1}$$

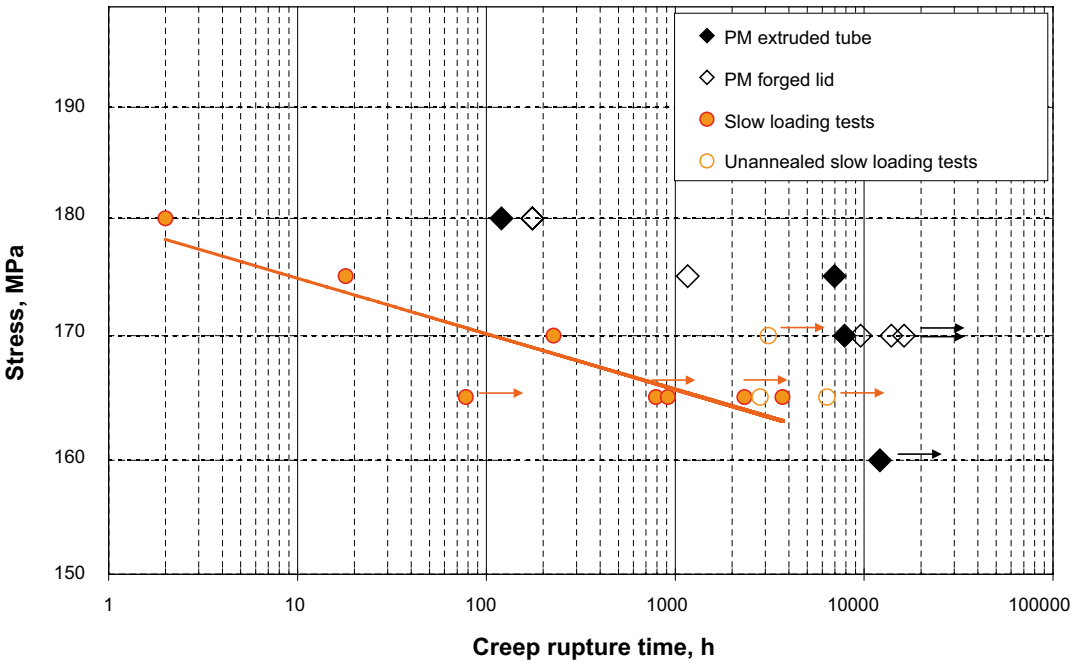

Figure 3-1. *Time to creep rupture given against applied stress. Previous results from traditional testing are included in the graph, marked PM [6]. Arrows identify tests that are still running.*

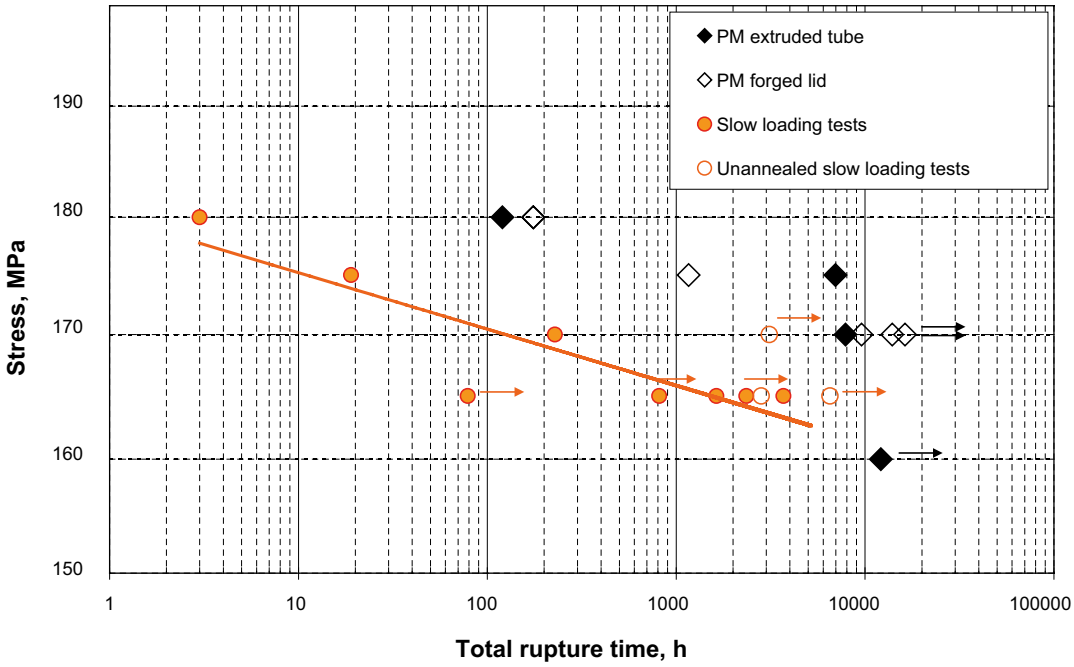

Figure 3-2. *Same as Figure 3-1 with the time representing the total rupture time, i.e. including the loading time.*

Table 3-1. Test matrix and creep test results.

Test ID	Material	Temp. [°C]	Stress [MPa]	Loading time [h]	Time [h]	Total time [h]	Loading strain [%]	Creep strain [%]	Total strain [%]	Measured strain on specimen [%]	Area red [%]	Min creep rate [%/h]	Status
Anneal 1	Lid annealed	75	180	1	2	3	16.9	17.1	34.0	49.6	92.0	6.52	Ruptured
Anneal 2		75	175	1	18	19	23.8	14.6	38.4	46.8	90.1	0.45	Ruptured
Anneal 3		75	170	1	227	228	23.2	21.4	44.6	49.0	61.6*	0.0335	Ruptured
Anneal 4		75	165	1	77.8	78.8	16.1	10.1	26.2	46.6	68.6*	–	Interrupted
Anneal 7		75	165	1	3,695	3,696	19.5	21.2	40.7	48.0	66.3*	0.00025	Ruptured
Anneal 8		75	165	24	790	814	26.2	10.8	37.0	51.7	89.7	–	Interrupted
Anneal 5		75	165	24	2,326	2,350	23.2	19.0	42.2	48.4	38.7*	0.00462	Interrupted
Anneal 11		75	165	719	914	1,633	25.4	14.9	40.3	51.4	63.7*	0.01198	Ruptured
Anneal 9		75	165	2,160	1,320	3,480	30.0	16.1	46.1	53.4	66.4*	0.00159	Ruptured
Anneal 10		75	165	4,320	814	5,134	33.9	17.7	51.6	51.9	63.9*	0.01215	Ruptured
Unanneal 1	Lid unannealed	75	170	1	3,114	3,115	8.8	10.1	18.9	19.3	–	–	Interrupted
Unanneal 2		75	165	1	2,816	2,817	5.7	14.5	20.2	21.9	–	0.0008	Ruptured
Unanneal 3		75	165	168	6,358	6,526	10.6	6.5	17.1	19.0	–	–	Interrupted

* Specimen did not rupture, the test rig stopped at 70% load drop.

The creep ductility is given in Figure 3-3 and Figure 3-4. It is evident from the graphs that the total strain is comparable to previous work. In the previous work loading strains of about 10% were found [6]. In the present work the unannealed specimens show similar strains, Table 3-1, but none of the slow loading experiments shows less than 16% loading strain. The highest loading strain is noted for the 6 months loading tests which exhibits a loading strain of over 33%. Included in this is the creep strain experienced as the test approaches the maximum load, which accounts for the additional strain.

In Figure 3-5 the loading process has been plotted against normalised time (time divided by total loading time). This allows for the study of radically dissimilar loading times in the same graph. It is shown that the loading strain increases with increasing loading time. At the same time the total strain is similar for all tests, Table 3-1. The increase in loading strain it thus balanced by a similar decrease in creep strain. Illustrative of this is the creep curves given in Figure 3-6 to Figure 3-8. The curves show that all of the specimens reach roughly the same total strain but that the creep part is decreased when the loading stage is increased. Tempory instabilities in testing were sometimes observed, see for example Figure 3-7.

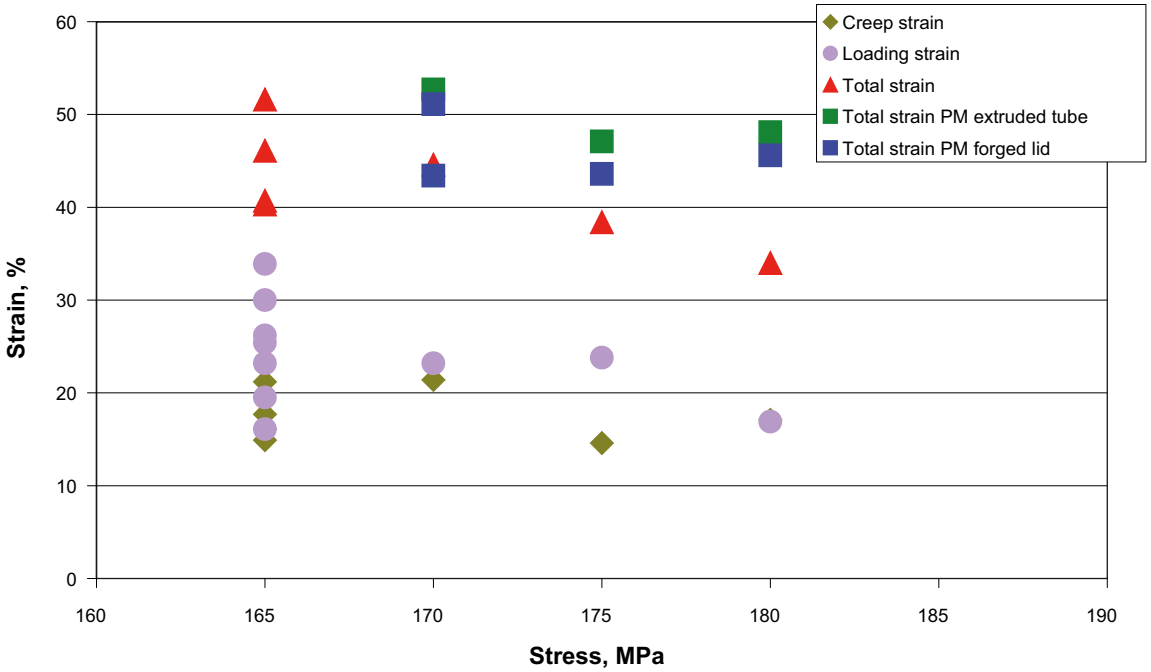

Figure 3-3. *Strain as a function of applied stress. Loading strain, creep strain and total strain is separated for the tests in this investigation. Test results marked PM are taken from [6].*

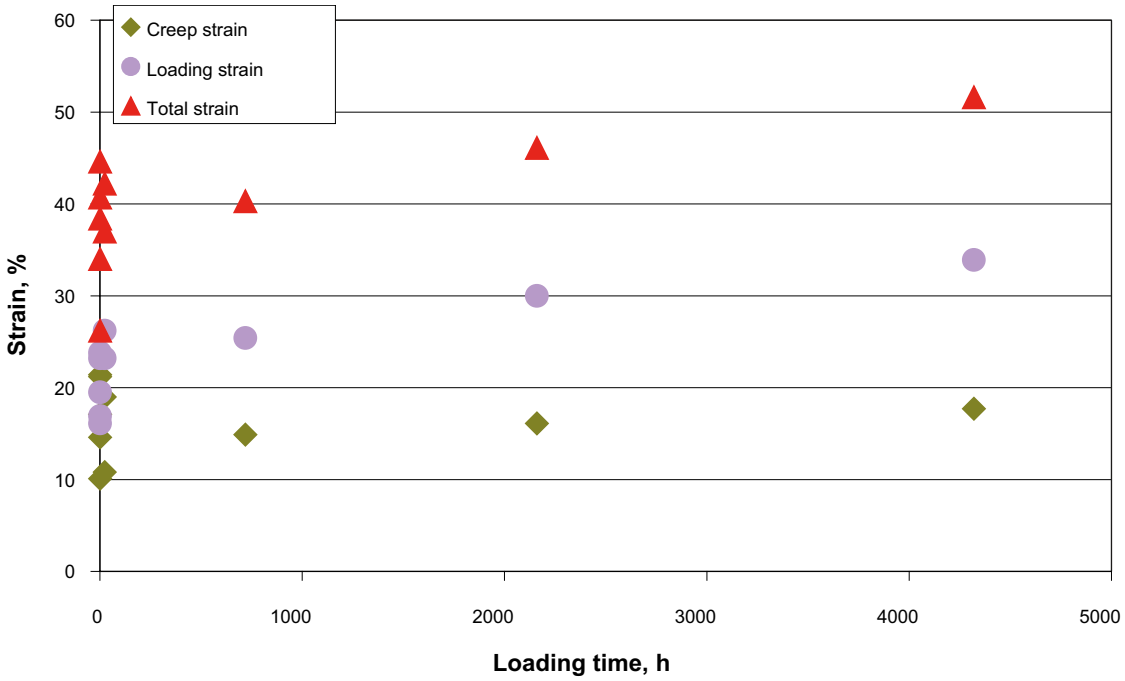

Figure 3-4. *Strain as a function of loading time. The strain increases as the loading time increases.*

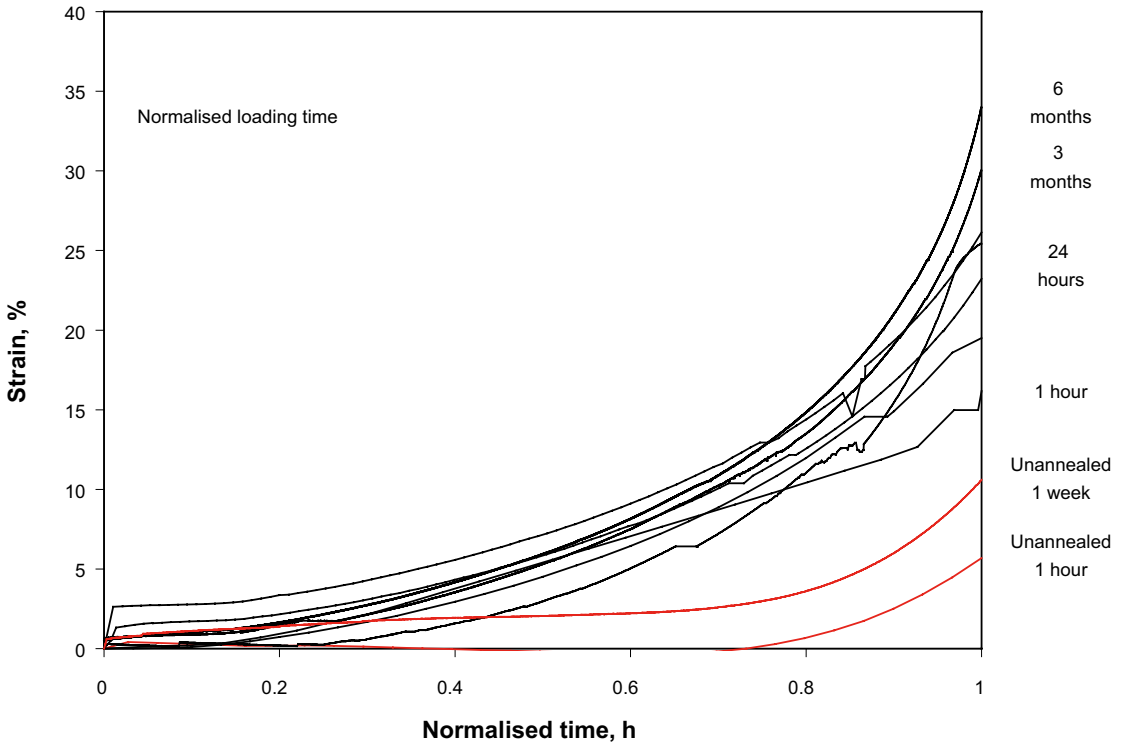

Figure 3-5. *The loading strains for the slow loading tests given against normalised time (time divided by total loading time).*

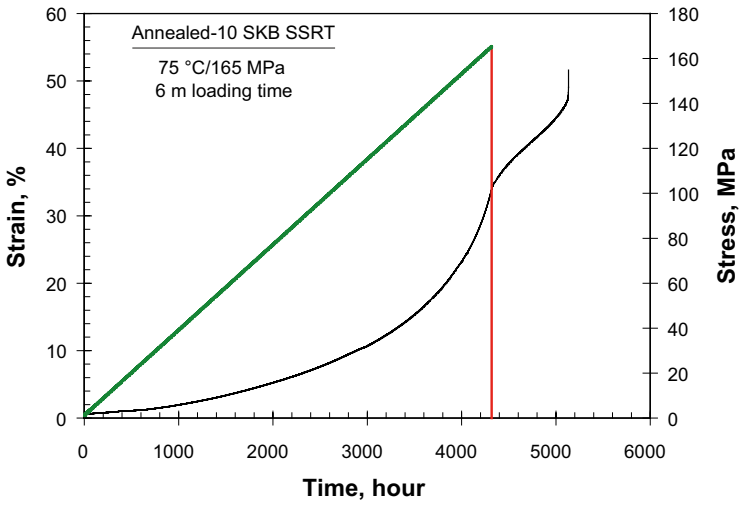

Figure 3-6. *Loading and creep stage of a specimen tested at 165 MPa; loading time 6 months.*

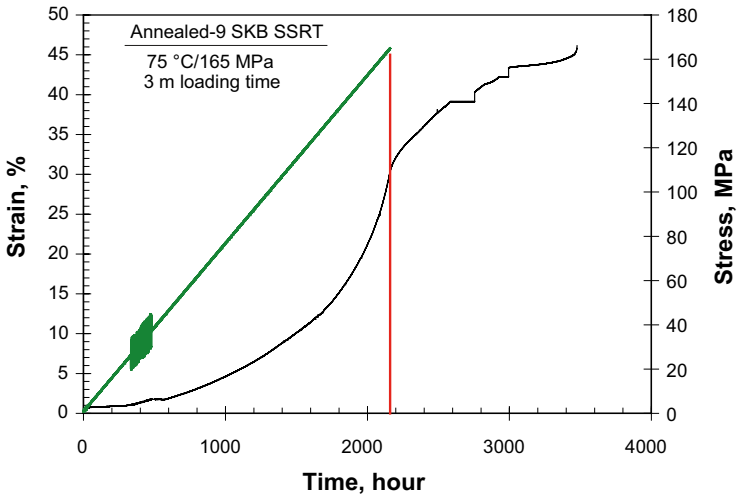

Figure 3-7. *Loading and creep stage of a specimen tested at 165 MPa; loading time 3 months.*

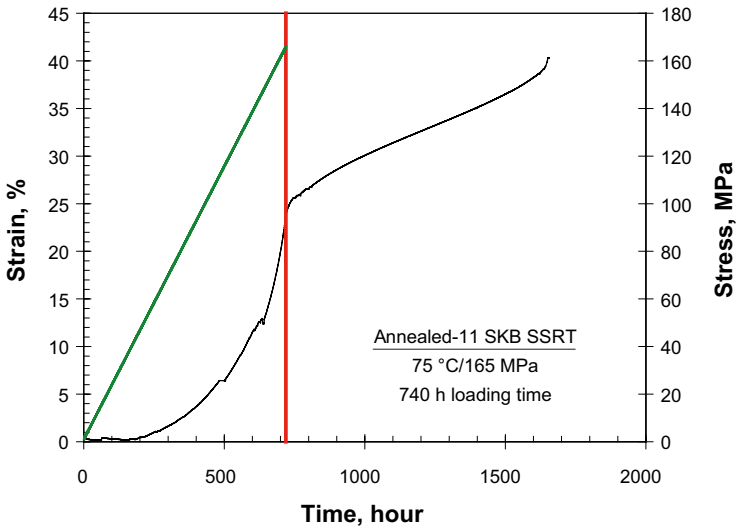

Figure 3-8. *Loading and creep stage of a specimen tested at 165 MPa; loading time 1 month.*

4 Model

During the creep testing there are two contributions to the straining. First there is an essentially time independent athermal plastic deformation. Second there is creep deformation. Traditionally the plastic deformation is measured in tensile tests and the creep deformation in constant load creep tests. There is no fundamental difference between the two types of deformation, but it is practical to distinguish between them during modelling because the two parts can then be verified experimentally.

4.1 Athermal plastic deformation

Tensile flow curves in Cu-OFP can accurately be described with the help of Kocks-Mecking equation

$$\sigma = \sigma_y + B(1 - e^{-\omega\varepsilon/2}) \tag{4-1}$$

where σ is the stress and ε the strain, and σ_y the yield strength. The constants B and ω can be derived from basic dislocation relationships [7]: $\omega = 14.66$ and B is approximately 169 MPa at 75°C. σ_y is given the value 70 MPa [7]. In the creep tests the stress first increases linearly with time t and is the constant equal to the applied stress σ_{appl}.

$$\sigma = \sigma_{appl}\frac{t}{t_{load}} \qquad t < t_{load}; \qquad \sigma = \sigma_{appl} \qquad t \geq t_{load} \tag{4-2}$$

With the help of Equation 4-1 the plastic strain can be obtained

$$\varepsilon_{pl} = -\frac{2}{\omega}\log(1 - (\sigma - \sigma_y)/B) \tag{4-3}$$

From 4-3 we can derive an expression for the time derivative of the plastic strain

$$\frac{d\varepsilon_{pl}}{dt} = \frac{2}{\omega(B - (\sigma - \sigma_y))}\frac{d\sigma}{dt} \tag{4-4}$$

If Equation 4-2 is inserted into 4-4, an explicit time dependence is obtained that can be used to find the plastic strain as a function of time.

4.2 Primary and secondary creep

A model for the stationary creep rate has previously been derived [8]

$$\dot{\varepsilon}_{OFP} = h(\sigma, T) = \frac{2bc_\rho}{m}\frac{D_{s0}b\tau_L}{k_B T}\left(\frac{\sigma}{\alpha m G b}\right)^3 e^{\frac{\sigma b^3}{k_B T}} e^{-\frac{Q}{RT}\left[1-(\frac{\sigma}{\sigma_{i\max}})^2\right]} / f_P \tag{4-5}$$

The interpretation of the parameters can be found in the published paper or in [2].

Taking the dependence of the strain rate $\dot{\varepsilon}$ into account in Equation 4-1, it can be expressed as

$$\sigma = (\sigma_y + B(1 - e^{-\omega\varepsilon/2}))(\frac{\dot{\varepsilon}}{\dot{\varepsilon}_0})^{1/n} \tag{4-6}$$

where $\dot{\varepsilon}_0$ is a reference strain rate and n the Norton exponent that can be determined from Equation 4-5. By rearranging Equation 4-6, an expression for the strain rate is obtained

$$\dot{\varepsilon} = \dot{\varepsilon}_0(\frac{\sigma}{\sigma_y + B(1 - e^{-\omega\varepsilon/2})})^n \tag{4-7}$$

Equation 4-7 will be used to describe primary and secondary creep. The value of $\dot{\varepsilon}_0$ is chosen by ensuring that $\dot{\varepsilon}$ reaches the stationary creep rate at larger strains. By using Equation 4-5 for the stationary strain rate, the following relation is obtained for $\dot{\varepsilon}_0$ from 4-7.

$$h(\sigma,T) = \dot{\varepsilon}_0 (\frac{\sigma}{\sigma_y + B})^n \quad (4\text{-}8)$$

Combining Equation 4-7 and Equation 4-8, the desired expression for the creep rate is found

$$\dot{\varepsilon} = h(\sigma,T)(\frac{\sigma_y + B}{\sigma_y + B(1 - e^{-\omega\varepsilon/2})})^n \quad (4\text{-}9)$$

Since the stress corrections has the same form as in the Norton equation, they can be moved inside the brackets

$$\dot{\varepsilon} = h(\sigma \frac{\sigma_y + B}{\sigma_y + B(1 - e^{-\omega\varepsilon/2})}, T) \quad (4\text{-}10)$$

Equation 4-10 is the preferred formulation. However, Equation 4-9 gives numerically almost the same results. Equation 4-10 or Equation 4-9 represents an expression for primary and secondary creep rate based on the function $h(\sigma, T)$ in Equation 4-5 [9].

4.3 Influence of cold work

The reason for annealing the majority of specimens was that a small amount of cold worked was expected to be present in the lid material from which the specimens were extracted. We assume that the material has been exposed to a cold work strain of ε_{cw}. According to Equation 4-1 the flow stress can be then be expressed as

$$\sigma = \sigma_y + B(1 - e^{-\omega(\varepsilon + \varepsilon_{cw})/2}) \quad (4\text{-}11)$$

Alternatively this equation can be rewritten in the following way with new values of σ_y and B

$$\sigma = \sigma_{ycw} + B_{cw}(1 - e^{-\omega\varepsilon/2}) \quad (4\text{-}12)$$

where

$$B_{cw} = Be^{-\omega\varepsilon_{cw}/2} \qquad \sigma_{ycw} = \sigma_y + B - B_{cw} \quad (4\text{-}13)$$

For the creep rate a back stress σ_b must also be introduced

$$\dot{\varepsilon} = h((\sigma - \sigma_b)\frac{\sigma_y + B}{\sigma_y + B(1 - e^{-\omega(\varepsilon + \varepsilon_{cw})/2})}, T) \quad (4\text{-}14)$$

The back stress can be related to the dislocation density ρ_{cw} introduced by the cold working

$$\sigma_b = m\alpha Gb\rho_{cw}^{1/2} \quad (4\text{-}15)$$

The dislocation density will be gradually reduced due to dynamic recovery [7]

$$\frac{d\rho}{d\varepsilon} = -\omega\varepsilon \quad (4\text{-}16)$$

Integrating Equation 4-16 gives

$$\rho_{cw} = \rho_{cw}^0 e^{-\omega\varepsilon} \quad (4\text{-}17)$$

The initial dislocation density can be related to the change in yield strength

$$\sigma_{ycw} - \sigma_y = m\alpha Gb(\rho_{cw}^0)^{1/2} = B(1 - e^{-\omega\varepsilon_{cw}/2}) \quad (4\text{-}18)$$

The last member follows from Equation 4-13. The final expression for σ_b is obtained by inserting Equation 4-17 and Equation 4-18 into Equation 4-15

$$\sigma_b = B(1 - e^{-\omega\varepsilon_{cw}/2})e^{-\omega\varepsilon/2} \quad (4\text{-}19)$$

4.4 Comparison to experiments

The total strain rate is obtained by adding the athermal plastic strain rate in Equation 4-4 and the creep strain rate in Equation 4-14

$$\frac{d\varepsilon}{dt} = \frac{d\varepsilon_{pl}}{dt} + \frac{d\varepsilon_{c}}{dt} \tag{4-20}$$

The development of the strain during the creep tests can then be found by integration of Equation 4-20. In Figure 4-1 experimental results are compared to the model when the loading time is short, 1 h.

The model gives a reasonable representation of the experiments. During the loading the athermal plastic strain gives the dominating contribution, but it is unchanged in the constant load stage.

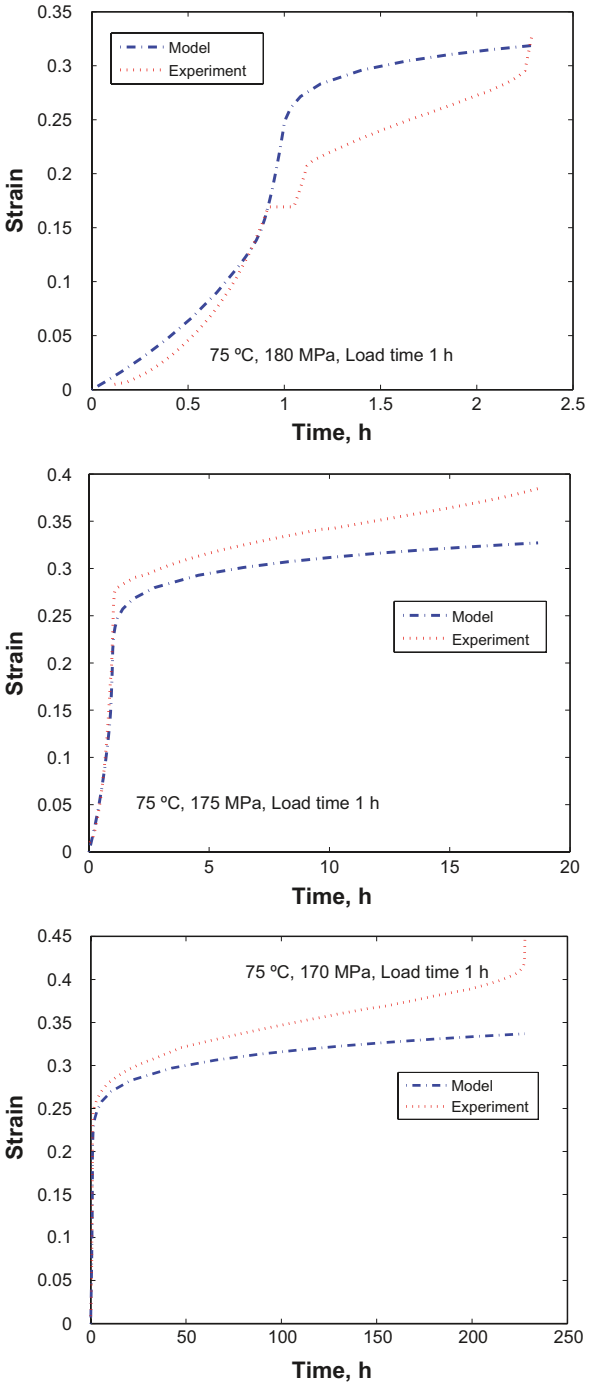

Figure 4-1. *Creep strain versus time for three tests with 1 h loading time. Specimens Anneal 1, 2, and 3.*

Figure 4-2 shows that the time to rupture increases with loading time. This is natural since until the load is close to the constant level, the development of creep damage is negligibly small. In fact, the difference between the rupture time and the loading time is of the order of 1,000 h for all three specimens in Figure 4-2, which have been tested at the same final applied stress of 165 MPa. The scatter in creep data is however large. This is illustrated by specimen Anneal 7 that for the same applied stress had a rupture time of 3,696 h after a loading time of 1 h.

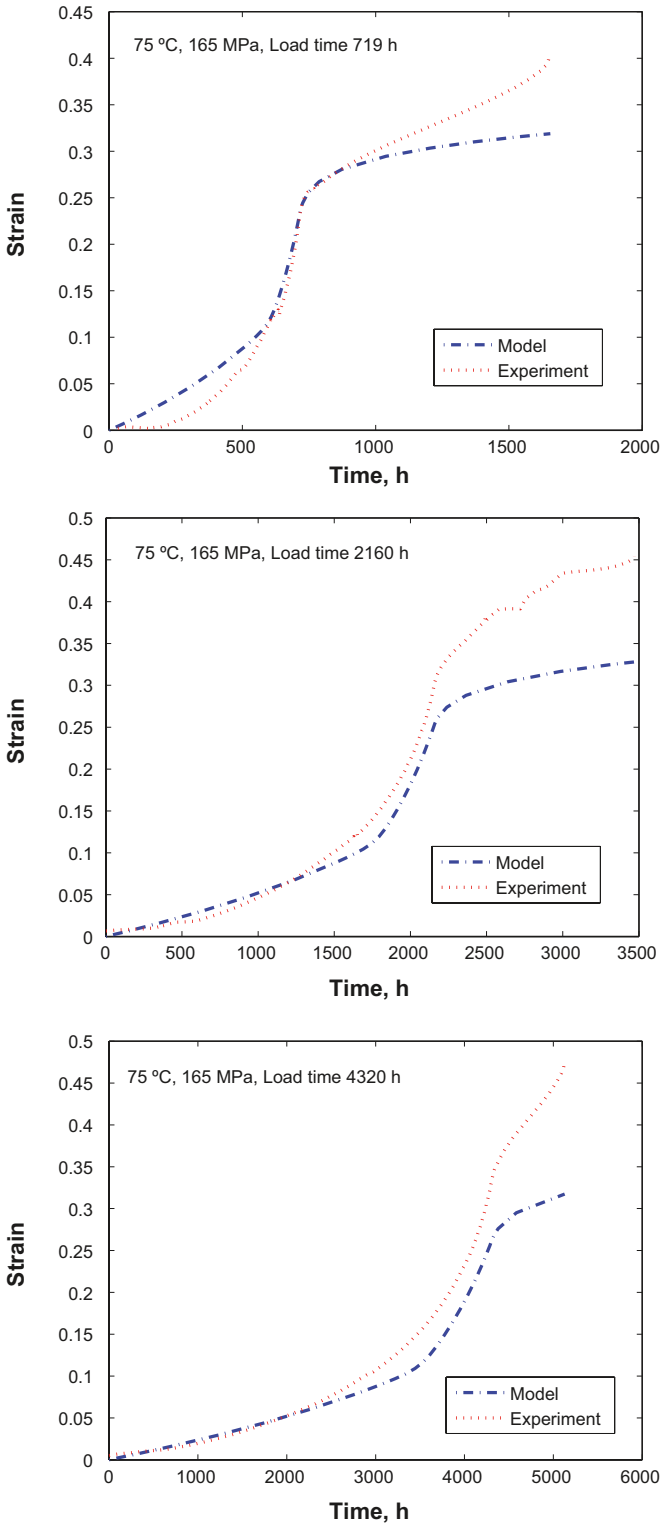

Figure 4-2. *Creep strain versus time for three tests with 1 h loading time. Specimens Anneal 11, 9, and 10.*

The results in Figure 4-1 and Figure 4-2 represent specimens that have been annealed before testing. In Figure 4-3 and Figure 4-4, comparisons are made between annealed and unannealed specimens. It is evident that both the initial loading strain as well as the creep strain rate are much higher for the annealed material. This is believed to be due to the presence of cold work in the lid where the specimens have been taken from. During annealing this cold work has been removed.

In the model the influence of cold work has been taken into account by assuming that $\varepsilon_{cw} = 0.02$, i.e. 2% cold work. Since the amount of cold work has not been measured this figure should be considered as an estimate.

In Figure 4-5 data from a previously studied lid (lid 1) are compared to the results in the present investigation (lid 2). All the tests in Figure 4-5 are for unannealed material. In the model $\varepsilon_{cw} = 0.01$ and $\varepsilon_{cw} = 0.02$ have been assumed for lid 1 and 2, respectively. There are technical reasons for this difference, since the workshop handling of the two lids was not identical and more cold work was expected in lid 2 material. That was one of the reasons for annealing most of the specimens.

In Figure 4-5 the creep rate increases with increasing stresses and decreasing amount of cold work. The model can represent this kind of behaviour.

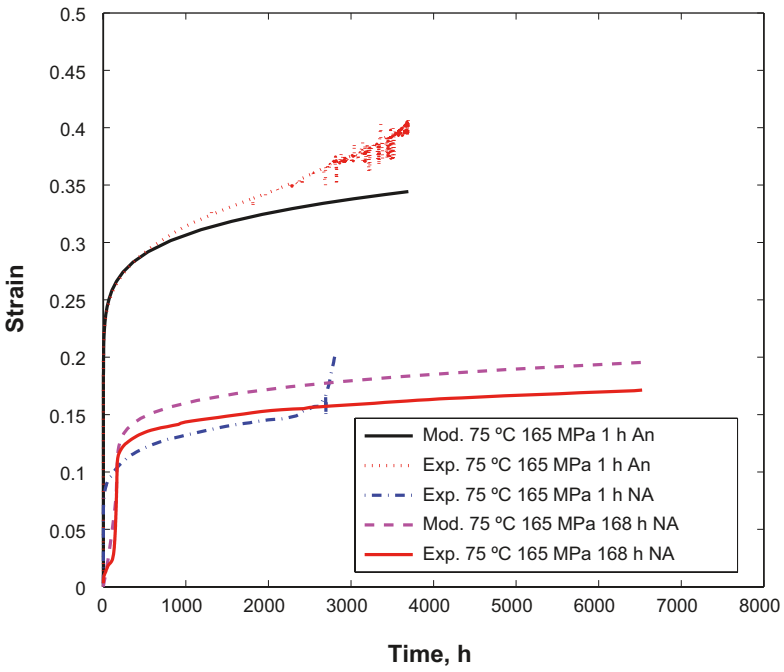

Figure 4-3. *Comparison of creep tests between annealed and unannealed specimens. Specimens Anneal 4 and Unanneal 2 and 3. In the model for the unannealed specimens,* $\varepsilon_{cw} = 0.02$ *has been assumed.*

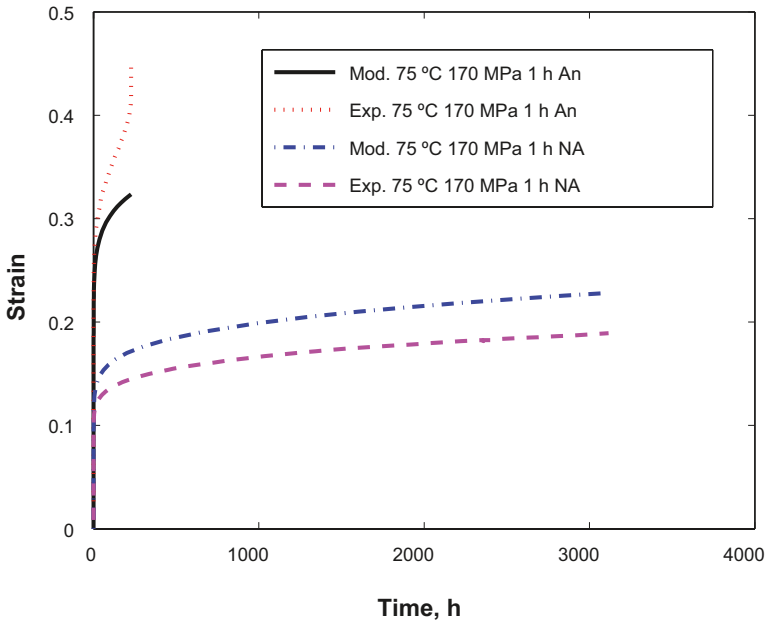

Figure 4-4. *Creep strain versus time for two tests with 1 h loading time. Comparison between annealed and unannealed specimens. Specimens Anneal 3 and Unanneal 1. In the model for the unannealed specimen,* $\varepsilon_{cw} = 0.02$ *has been assumed.*

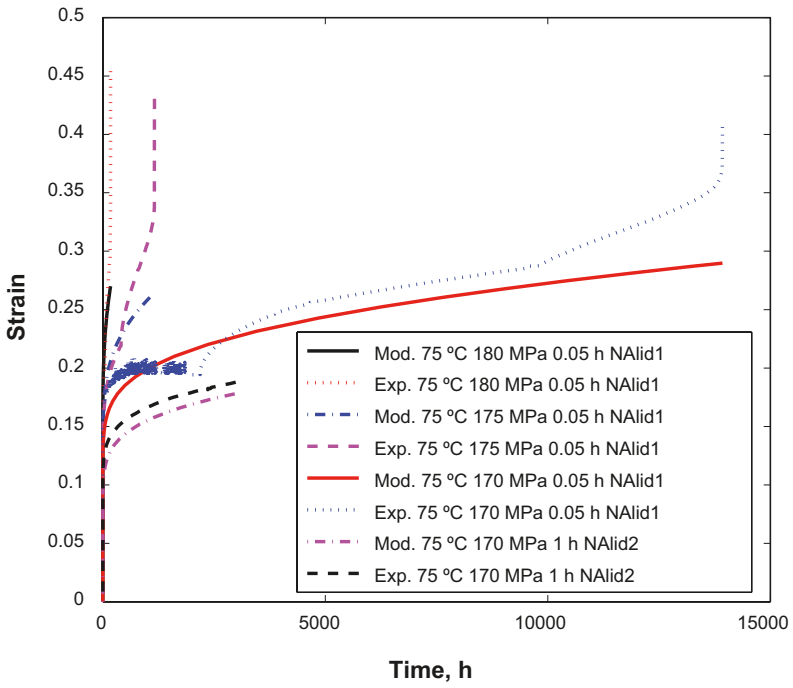

Figure 4-5. *Creep strain versus time for unannealed specimens. Three tests from [6] marked NAlid1 are included for comparison. Specimens Unanneal 1 and 2 (marked NAlid2). In the model* $\varepsilon_{cw} = 0.01$ *and* $\varepsilon_{cw} = 0.02$ *have been assumed for lid 1 and 2.*

5 Discussion

The rate at which the load is applied to a copper creep test affects the total result. The total ductility is not increased significantly but the ductility is moved from creep strain towards loading strain. That the total strain or ductility is not increased is perhaps not surprising since the straining mechanisms are the same in both cases. At 75°C the creep elongation is primarily controlled by plastic instability rather than the formation of creep damage. The ability does not change with the manner of the application of load and consequently the total ductility does not change.

The shift towards more loading strain is important. It means that the strain is accumulated earlier in the creep life. For instance the strain in the loading stage begins to accumulate earlier than creep tests performed at the same load would indicate. This can be observed for example from the 3 months loading experiment shown in Figure 3-7. This specimen reached a loading strain of 10% for 115 MPa, and 15% for 135 MPa. Neither load would cause creep in the copper when tested in the traditional way, but still the loading strain is significant. This is clearly athermal plastic strain.

This means that when a canister is placed in the final repository the deformation due to hydrostatic pressure will start at a lower load than traditional creep testing suggests and as a consequence the strain will be higher at a given time. If a stationary state is reached the total strain is not affected.

Another feature of the new continuous load creep test rigs is the maximum stroke which has been increased from 5 mm to approximately 50 mm. This has meant that it is possible to conduct testing until rupture without having to regularly unload and reset the specimen. It is not known how the creep life is affected by repeated unloading, see Figure 5-1. The "new" primary stages represent a plastic deformation and work hardening may increase the creep life.

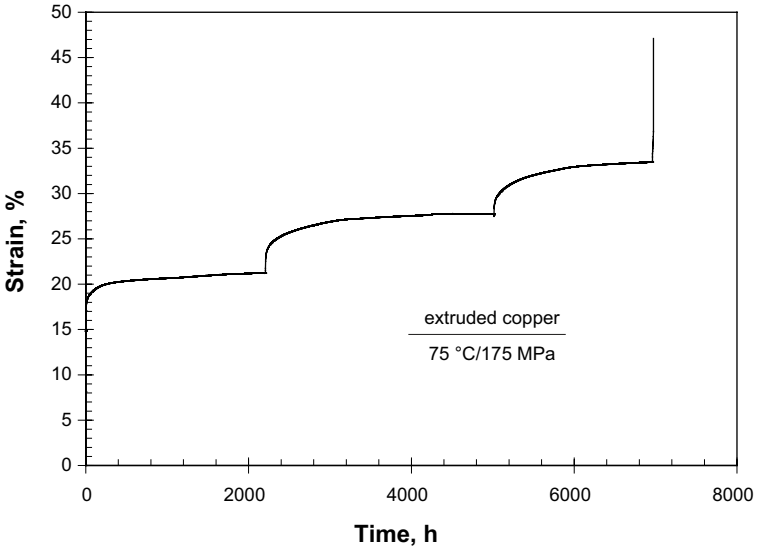

Figure 5-1. *Example of "renewed primary" creep in specimens unloaded for resets. This particular specimen was reset three times and ruptured during the last reset.*

Traditional creep testing differentiates between loading strain and creep strain. This is not critical when testing standard engineering materials such as ferritic steels. For these body centred cubic (bcc) materials the loading strain is usually less than 2% and the creep strain can be more than 10–20%. For steels it is not always customary to report the loading strain since it is small in relation to the total strain. The loading strain is thus neglected and in published texts on creep testing of steels total strain and creep strain are often used interchangeably. For copper in oxygen free form at temperatures from 75 to 175°C, the loading strain in traditional testing is 6–10%. The creep strain adds another 25–30% to a total strain of 40% or more. It is therefore vital to distinguish between loading and creep strain. This is uncomplicated when loading a test in a traditional way, all strain experienced before total application of the creep load is loading strain, and all strain thereafter is creep strain. The loading takes 2–5 minutes to perform and the material will not creep significantly in this timescale. All deformation can be viewed as plastic deformation. In a continuously loaded test where the loading phase is weeks or more this distinction is much more complicated. The total strain is around 45% for more or less all tests. For those tests loaded in an hour or less the view might be taken that all strain experienced before total load is loading strain, in conjunction with traditional creep testing. But loading times of 3–6 months still show similar loading strain and yet they experience creep in the latter stages of the loading process since the load is large enough. The division between loading (plastic) strain and creep strain for these specimens is important to the interpretation of the tests and should be studied further.

6 Conclusions

Continuous loading creep test rigs with electro-mechanical motors have been developed. Creep tests for copper specimens at 75°C have been performed for loading times between 1 and 4,000 h. During the loading the stress increased linearly with time.

- The total strain including loading strain was found to be 30–50%, similar to previous experience with short loading times.
- For longer loading times, the loading strain increased at the expense of the creep strain.
- The largest loading strain was found to be 33%, probably including a significant amount of creep strain.
- The relation between creep strain and loading strain at low stresses should be studied further.
- A model has been developed for the mainly athermal plastic strain during loading. At the final stages of the loading and during the constant load phase, creep straining is of importance. The model is able to describe the two contributions to the plastic deformation as a function of time.

7 References

SKB's (Svensk Kärnbränslehantering AB) publications can be found at www.skb.se/publications.

1 **SKB, 2010.** RD&D Programme 2010. Programme for research, development and demonstration of methods for the management and disposal of nuclear waste. SKB TR-10-63, Svensk Kärnbränslehantering AB.

2 **Andersson-Östling H C M, Sandström R, 2009.** Survey of creep properties of copper intended for nuclear waste disposal. SKB TR-09-32, Svensk Kärnbränslehantering AB.

3 **Raiko H, Sandström R, Rydén H, Johansson M, 2010.** Design analysis report for the canister. SKB TR-10-28, Svensk Kärnbränslehantering AB.

4 **ISO/DIS 204:2005.** Metallic materials – Uniaxial creep testing in tension – Method of test, European Standard Draft prEN ISO 204. Brussels: European Committee for Standardization.

5 **Henderson P J, Lindblom J, 1995.** Results of round-robin tensile testing and effect of specimen diameter on the tensile and creep properties of high-purity copper. Progress Report 95-2, Swedish Institute for Metals Research.

6 **Andersson H C M, Seitisleam F, Sandström R, 2007.** Creep testing and creep loading experiments on friction stir welds in copper at 75°C. SKB TR-07-08, Svensk Kärnbränslehantering AB.

7 **Sandström R, Hallgren J, Burman G, 2009.** Stress strain flow curves for Cu-OFP. SKB R-09-14, Svensk Kärnbränslehantering AB.

8 **Sandström R, Andersson H C M, 2008.** Creep in phosphorus alloyed copper during power-law breakdown. Journal of Nuclear Materials 372, 76–88.

9 **Wu R, Seitisleam F, Sandström R, 2009.** Creep properties of phosphorus alloyed oxygen free copper under multiaxial stress state. SKB R-09-41, Svensk Kärnbränslehantering AB.